Mathematical Model for River Ice Processes

By A. M. Wasantha Lal,[1] Associate Member, ASCE, and Hung Tao Shen,[2] Member, ASCE

Abstract: A computer model RICE is developed for simulating ice processes in rivers. In the river-hydraulics component, the flow condition is determined from one-dimensional unsteady flow equations. In the thermal component, distributions of water temperature and ice concentration are determined from transport equations of thermal energy and ice. Effects of surface ice, skim-ice, and border ice formations on the ice production are considered. The formation of ice cover is formulated according to existing equilibrium ice-jam theories, with consideration to the interaction between the ice cover and the flow. The undercover ice accumulation is formulated according to the critical velocity criteria. The thermal growth and decay of the ice cover is simulated using a finite-difference formulation applicable to composite ice covers consisting of snow, ice, and frazil layers.

Introduction

River ice undergoes processes of formation, evolution, transport, dissipation, and deterioration. These processes are not only affected by atmospheric conditions and river geometry, they also interact with the river flow. Many river ice processes are not yet well understood. However, by utilizing existing theories, a mathematical model of these processes can be developed. Such a model can be used to provide a continuous description of river ice development based on a limited amount of field data. The model can also assist engineers in evaluating the possible beneficial and detrimental consequences of ice-control structures and flow regulation.

In recent years a number of river ice models (e.g., Petryk et al. 1981; Calkins 1984; Shen and Yapa 1984) have been developed for rivers with floating ice covers. All of these models simulate river ice processes with various degrees of simplifications in the analytical formulation. In this paper, the development of a more comprehensive model RICE (Lal 1989; Lal and Shen 1990) is presented.

River Ice Processes

At the beginning of winter, due to the heat loss from the water surface, water temperature in the river can drop to the freezing point. Further cooling will lead to ice formation. In slow-flowing areas of the river, the turbulence intensity is not strong enough to mix the cold water or frazil crystals over the depth. Static ice in forms of stationary or moving skim ice can develop in these areas before the average water temperature of the cross section drops to the freezing point. In fast-flowing areas of the river, frazil ice crystals

[1]Res. Engr., Dept. of Civ. and Envir. Engrg., Clarkson Univ., Potsdam, N.Y. 13699-5710.

[2]Prof., Dept. of Civ. and Envir. Engrg., Clarkson Univ., Potsdam, N.Y.

Note. Discussion open until December 1, 1991. To extend the closing date one month, a written request must be filed with the ASCE Manager of Journals. The manuscript for this paper was submitted for review and possible publication on April 3, 1990. This paper is part of the ***Journal of Hydraulic Engineering***, Vol. 117, No. 7, July, 1991. ©ASCE, ISSN 0733-9429/91/0007-0851/$1.00 + $.15 per page. Paper No. 25948.

mix over the depth due to turbulence, grow in size, multiply in number and agglomerate into flocs. When the frazil particles and flocs grow in size, they will float to the river surface to form a layer of surface ice. The concentration in the surface layer is usually much higher than the concentration of the ice remaining in suspension.

The continuous increase in the surface ice concentration may lead to the formation of ice pans. Ice pans grow in size and strength when they travel along the river due to the freezing of interstitial water and further accumulation of frazil ice both around the circumference and on the underside of pans. Ice pans may either sinter into still larger ice floes if they travel over a long distance or break into fragments when passing through rapid sections. Partial coverage of the water surface by the moving surface ice layer results in a reduction of the net ice production due to the insulating effect. The downstream transport of the surface ice will cease when it reaches an artificial obstacle or a river section where an ice bridge across the river is formed by the congestion of the surface ice. Once an obstacle is reached, the incoming surface ice will accumulate on its upstream side and extend the ice cover upstream. Frazil ice remaining in suspension will continue to be transported downstream and be deposited on the underside of the ice cover.

The phenomena of ice bridging is not well understood, even though ice bridges often form at the same location each winter. The formation of an ice bridge in a river reach is related to its ice-transport capacity and the rate of ice supply from upstream. The maximum rate of ice discharge that can pass through a river section while not forming an ice bridge depends on the flow velocity, the channel top width between banks or border ice boundaries, the surface slope, the weather conditions, as well as the size, concentration and material properties of the ice in the surface layer (Matousek 1988; Shen et al. 1990).

Once an ice cover is initiated, it may progress upstream through the accumulation of incoming surface ice. The rate of progression of the leading edge of an ice cover depends on the rate of surface ice supply and the thickness of the new ice cover. The cover thickness is governed by the flow condition at the leading edge. When the flow velocity is relatively low, incoming surface ice will accumulate into a smooth single-layer ice cover in the form of juxtaposition. During the freezing-up period, if the surface ice consists mainly of highly deformable frazil slush or loose frazil pans, the juxtaposition mode may not be clearly identifiable due to the compression of the surface ice elements. At a higher velocity, surface ice elements can underturn or submerge at the leading edge to form an ice cover of larger thickness. This mode of ice-cover formation by hydraulic thickening is often called "narrow jam" (Pariset and Hausser 1961). In this mode, there exists a limiting cover thickness and a corresponding flow velocity. When this velocity is exceeded, ice particles are swept under at the leading edge. This leads to the cessation of the leading-edge progression, until flow velocity at the leading edge is reduced. This reduction in velocity can be caused by either a reduction in river discharge or the backwater effect induced by the increase in undercover ice accumulation.

A cover has to be thick enough so that the ice cover is capable of withstanding the net force acting on it. Forces acting on the cover include wind and water drags, and the weight of the ice cover, counterbalanced by the bank shear. If the strength of the ice cover together with the bank shear

cannot support external forces acting in the streamwise direction, mechanical thickening or shoving will occur until the cover reaches a thickness capable of withstanding the external forces. The freeze-up of a thin layer of solid ice from the interstitial water in the granular surface ice accumulation can significantly increase the strength of the initial ice cover.

The surface ice that is swept under the ice cover can travel along the underside of the ice cover and be deposited downstream. The frazil ice that was in suspension when entering the ice-covered region can rise to the underside of the cover and contribute to this process. Undercover ice depositions are called hanging dams or frazil ice jams. They are often observed to occur under ice covers downstream of rapids. If the flow velocity increases at a later period, loosely accumulated ice on the underside of the cover can be eroded and transported farther downstream.

This discussion is presented in the context of ice-cover formation during freeze-up. Similar processes can occur when a large quantity of surface ice pieces is released due to breakup of ice covers upstream. In this case the leading edge of the intact downstream ice cover often acts as the obstacle that initiates the surface ice accumulation process.

With heat loss through a newly consolidated ice cover, water-filled voids in the granular ice mass will freeze from the water level downward. This process is faster than black-ice growth. The existence of a snow cover can also affect the thermal growth of the ice cover. The snow cover provides an insulation layer that can retard the thermal growth of the ice cover. However, when the snow-ice interface submerges below the water level, the snow-ice growth leads to a faster growth of the ice-cover thickness.

Model Formulation

The major components included in the present model are: (1) The hydraulics of river flow; (2) the water temperature and ice concentration distributions; (3) the ice-cover formation including border ice formation and the formation of the main ice cover; (4) the undercover transport and accumulation; (5) the thermal growth and decay of ice cover; and (6) the stability of ice cover under the influence of hydromechanical forces. The effects of both skim-ice formation and moving surface ice on ice production are considered. A two-layer formulation that distinguishes the surface ice run from the ice that remains in suspension is introduced in the simulation of ice transport and accumulation processes.

River Hydraulics

If the effect of phase changes on the conservation of water mass are neglected, stage and discharge variations in a river with a floating ice cover can be described by the following continuity and momentum equations:

$$\frac{\partial Q}{\partial x} + \frac{\partial A}{\partial t} = 0 \quad (1)$$

and

$$\rho \frac{\partial Q}{\partial t} + \rho \left(\frac{2Q}{A} \frac{\partial Q}{\partial x} - \frac{Q^2}{A^2} \frac{\partial A}{\partial x} \right) + \rho g A \frac{\partial H}{\partial x} + (p_i \tau_i + p_b \tau_b) = 0 \quad (2)$$

in which x = distance, t = time; g = gravity; Q = discharge; A = flow area; $H = z_b + d_w + h$, water level; z_b = bed elevation; d_w = depth of flow; h = submerged thickness of the ice cover; ρ, ρ_i = density of water and ice, respectively; p_b, p_i = wetted perimeters formed by the channel bed and the ice cover, respectively; and τ_b, τ_i = shear stresses at the channel bottom and at the ice-water interface; respectively. A four-point implicit finite difference scheme (Yapa and Shen 1986) is used to solve (1) and (2).

Simulation of the ice-cover geometry, including its thickness and area will be discussed in later sections. The flow resistance terms in (2) can be expressed in terms of Manning's coefficients of the channel bed n_b, and the ice cover n_i (Yapa and Shen 1986). The time-dependent variation of the ice-roughness coefficient from freeze-up to breakup is formulated as:

$$n_i = (n_{i,i} - n_{i,e})e^{-\alpha_n t} + n_{i,e} \qquad (3)$$

in which $n_{i,i}$ and $n_{i,e}$ = initial and end values of n_i; and α_n = a decay constant. Methods for selecting parameters in (3) have been discussed by Nezhikovskiy (1964) and Yapa and Shen (1986).

Water Temperature and Ice Concentration Distributions

In a one-dimensional analysis, the distribution of water temperature along a river can be described by the following transport equation:

$$\frac{\partial}{\partial t}(\rho C_p A T_w) + \frac{\partial}{\partial x}(Q\rho C_p T_w) = \frac{\partial}{\partial x}\left(AE_x\rho C_p \frac{\partial T_w}{\partial x}\right) - B_0\phi_T \qquad (4)$$

in which B_0 = river width between border ice; C_p = specific heat of water; E_x = dispersion coefficient; and ϕ_T = net rate of heat loss per unit surface area of the river. When water temperature drops below the freezing point, T_f, frazil ice will be produced. The equation for cross-section–averaged ice concentration distribution becomes (Shen and Chiang 1984):

$$\frac{\partial}{\partial t}(\rho_i L_i C_i) + \frac{\partial}{\partial x}(Q\rho_i L_i C_i) = \frac{\partial}{\partial x}\left(AE_x\rho_i L_i \frac{\partial C_i}{\partial x}\right) + B_0\phi_T + \Sigma S \qquad (5)$$

in which C_i = ice concentration; L_i = latent heat of fusion; ΣS = additional source or sink terms representing ice used for progression, undercover deposition and ice supply from the erosion of the undercover accumulation. Since (5) is in the same form of (4), the solution of (4) when $T_w < 0°$ C can be used to determine the ice concentration by letting $C_i = -(\rho C_p T_w)/(\rho_i L_i)$. Neglecting the dispersion term, (4) and (1) can be combined to give the following Lagrangian equation.

$$\frac{DT_w}{Dt} = \frac{B_0\phi_T}{\rho C_p A} \qquad (6)$$

Eq. (6) is solved using an Eulerian-Lagrangian scheme (Lal and Shen 1990). The net heat exchange includes heat exchanges at the water surface, channel bed, as well as the heat generated from viscous dissipation. In open-water reaches, ϕ_T may be approximated by the rate of surface heat loss, ϕ_{wa}, which can either be evaluated by a detailed heat exchange computation or by a linearized approximation (Ashton 1986):

$$\phi_{wa} = h_{wa}(T_w - T_a) \qquad (7)$$

For the northern United States, the value of the heat exchange coefficient h_{wa} is about 20 W m^{-2o} C^{-1}.

The effect of moving surface ice, which will reduce the amount of ice production, is not considered in (5). The formulation of this effect will be discussed in the section on ice-cover progression. Under ice-covered conditions, the turbulent heat exchange takes place at the ice-water interface and ϕ_T can be approximated by (Ashton 1986):

$$\phi_{wi} = h_{wi}(T_w - T_f) \qquad (8)$$

in which $h_{wt} = 1{,}622u^{0.8}d_w^{0.2}$ W m^{-2o} C^{-1}.

Skim-Ice Formation

The formation of skim ice is governed by the water surface temperature and the stability of frazil ice crystals formed on the water surface, both of these depend on the turbulence intensity. The formation of skim ice can have an important effect on the rate of frazil production. The theoretical formulation for this phenomenon is yet to be developed. An empirical formulation developed by Matousek (1984) is used. Based on the field observations in River Ohre, Matousek obtained an empirical relationship between water-surface temperature $T_{w,s}$, depth-averaged water temperature $T_{w,d}$, local depth-averaged flow velocity u, wind velocity V_a, and river surface width in the wind direction. Depending on the values of $T_{w,s}$ and $T_{w,d}$, different types of ice formation can occur. According to Matousek, the following criteria for ice formation may be used:

- When $T_{w,s} \geq 0°$ C, no ice phenomena will occur.
- When $T_{w,d} > 0°$ C, a skim-ice run will form if $T^c_{w,s} < T_{w,s} < 0°$ C and $V_b > v'_z$.
- When $T_{w,d} > 0°$ C, a skim-ice cover will form if $T_{w,s} < T^c_{w,s}$.
- When $T_{w,d} \leq 0°$ C, frazil-ice run will occur.

For these criteria, $T^c_{w,s}$ = a critical water-surface temperature; V_b = buoyant velocity of frazil ice; and v'_z = vertical component of turbulent fluctuations.

Border Ice Formation

The phenomena of border ice formation is not well understood. The empirical procedure discussed previously may be used to determine the static border formation. Svensson et al. (1989) developed a two-dimensional numerical model for static border ice formation. Based on comparisons with field data in the Lulea River, they suggested an empirical formulation for border ice formation. In the present model, Matousek's procedure discussed in the preceding section is used for consistency. In addition to the skim-ice mode, lateral progression of border ice can take place due to the accumulation or lodgment of surface elements. This type of lateral growth is limited by the stability of surface ice particles in contact with the edge of existing border ice. The rate of growth of the border ice width will be proportional to the surface concentration of the ice run. In the present model, the following empirical relationship obtained by Michel et al. (1982) is used:

$$R = 14.1V_*^{-0.93}N^{1.08} \qquad (9)$$

in which $R = (\rho L_i \Delta W)/(\Delta\phi)$; $V_* = u/V_c$; V_c = maximum velocity at which a surface ice particle can adhere to the border ice; ΔW = growth of border ice during a given time interval; $\Delta\phi$ = heat exchange per unit area during the given time interval; and N = area concentration of the surface ice discharge. According to Michel et al. (1982), the static mode of border ice formation exists when $N < 0.1$, and (9) can be used with $N = 0.1$. In the present study, since the static ice formation is modeled using Matousek's formulation, the lower limit for N is not used.

Michel et al. indicated that (9) is valid for $0.167 < V_* < 1.0$. When $V_* < 0.167$ static ice or skim-ice growth occurs; when $V_* > 1.0$ no surface ice can adhere to the border ice, the rate of border ice growth is negligible. The value of V_c varies with flow and ice conditions. It is determined by the stability of surface ice elements that are in contact with the edge of an existing border ice. The stability of an ice element is governed by the drag force acting on it including the component of the gravity force along the water surface and the hydrodynamic drag, which is resisted by the friction at the contact. For the Saint Anne River, the critical velocity V_c was found to be equal to 1.2 m/s (Michel et al. 1982). For the upper Saint Lawrence River, the V_c value is about 0.4 m/s (Shen et al. 1984). In the present one-dimensional model, transverse velocity distribution is not simulated. The limiting width of border ice growth is given as a model input for each reach based on the field observed critical velocity of 0.4 m/s.

Ice-Cover Progression

When ice run occurs, ice cover can be formed due to the bridging and accumulation of surface ice. This type of ice-cover formation is often called dynamic ice-cover formation. A complete dynamic ice-cover formation theory is yet to be developed (Shen et al. 1990). In this study, existing quasi-static formulation for surface ice accumulations (Pariset and Hausser 1961) together with free drift formulation for ice transport will be used. The bridging condition is considered an input based on site-specific empirical formulations.

The rate of ice-cover progression is governed by the rate of surface ice supply to the leading edge and the thickness of the new ice cover:

$$V_p = \frac{(Q_s^i - Q_u)V_s}{[B_0 h_0(1 - e_c)]V_s - (Q_s^i - Q_u)} \quad \text{(10)}$$

in which V_p = rate of cover progression of ice; $Q_s^i = \alpha C_i Q$, volumetric rate of surface ice discharge; Q_u = volumetric rate of surface ice swept under the cover at the leading edge; e_c = overall porosity of the cover, $e_p + (1 - e_p)e$; e = porosity of individual ice elements; e_p = porosity representing spaces in the accumulation between ice elements; h_0 = initial cover thickness; and V_s = velocity of the incoming surface ice, approximated by the current velocity. The coefficient α is the ratio between the total ice discharge $C_i Q$ and the surface ice discharge Q_s^i. A complete formulation of the evolution of surface ice discharge from a frazil ice run does not exist. A simplified formulation is developed in this study and summarized in Appendix I. This formulation, which can be used to determine Q_s^i and the suspended ice discharge Q_d^i, considers the transport of frazil suspension and surface ice run as a two-layer process with exchanges at the interface between these two layers.

The ice-cover progression can occur in three different modes. In regions with a low flow velocity, ice cover of one floe thickness can form by the juxtaposition of ice floes. In order for an ice cover to progress in this mode, a stability condition for incoming ice floes at the leading edge must be satisfied. According to Pariset and Hausser (1961), when the Froude number F_r at the leading edge is less than a critical value F_{rc}, the cover will progress in the juxtaposition mode. This critical Froude number can be expressed as:

$$\mathsf{F}_{rc} = f\left(\frac{t_i}{l_i}\right)\left(1 - \frac{t_i}{H}\right)\left[2\mathsf{g}\left(1 - \frac{\rho_i}{\rho}\right)(1 - e)\frac{t_i}{H}\right]^{1/2} \quad \text{(11)}$$

in which F_r = Froude number defined as $V/\sqrt{\mathsf{g}H}$; V and H = velocity and flow depth immediately upstream of the leading edge; t_i = ice floe thickness; $f(t_i/l_i)$ = a form factor that varies between 0.66 and 1.30; and l_i = length of the ice floe. Since no reliable method is available to determine the dimension of ice floes, field-observed values for F_{rc} are used in the present model. Based on field observations in the upper Saint Lawrence River, Shen, et al. (1984) suggested that the value of F_{rc} is between 0.05 and 0.06.

When F_{rc} is exceeded, the juxtaposition mode cannot exist, the cover will progress in the hydraulic-thickening or narrow-jam, mode. The initial cover thickness, h_0, in this mode of formation may be calculated by (Pariset and Hausser 1961):

$$\mathsf{F}_r = \left[2\frac{h_0}{H}(1 - e_c)\left(1 - \frac{\rho_i}{\rho}\right)\right]^{1/2}\left(1 - \frac{h_0}{H}\right) \quad \text{(12)}$$

From (12), one can show that there exists a maximum Froude number F_{rm}, beyond which the front of the cover cannot progress. Field observations by Kivisild (1959) suggested that F_{rm} varies between 0.05 and 0.1 with an average value of 0.08. Recent field studies indicated this value is approximately 0.09 (Shen et al. 1984; Sun and Shen 1988).

For wide steep river reaches, the increase in streamwise forces acting on the cover during its progression may exceed the increase in bank resistance. When the strength of the ice cover cannot resist the increase in stress due to the net streamwise force, the cover will collapse and thicken until an equilibrium thickness is reached (Pariset and Hausser 1961). This mode of cover formation through mechanical thickening is often referred to as the wide jam mode or shoving. For an equilibrium surface accumulation, the following force balance equation can be written.

$$2(\tau_c h_0 + \mu_1 f) = (\tau_i + \tau_g + \tau_a)B \quad \text{(13)}$$

in which f = longitudinal force in the cover; τ_i = shearing stress on the underside of the cover; τ_g = weight component of the cover along the water surface; ρ_a = density of air; $\tau_a = C_a\rho_a|V_a|V_a \cos\theta_a$ = wind stress along the cover; θ_a = angle between the wind direction and downstream direction of the river; C_a = resistance coefficient depending on surface roughness; μ_1 = a bank friction coefficient; and τ_c = cohesive component of the bank shear. Assuming complete mobilization of the granular mass, the balance between the passive resistance of the ice cover and the net longitudinal force f gives:

$$f = \rho_i K_2\left(1 - \frac{\rho_i}{\rho}\right)\frac{\mathsf{g}h_0^2}{2} \quad \text{(14)}$$

in which $K_2 = \tan^2(\pi/2 + \phi/2)(1 - e_c)$; $\tan \phi$ = internal friction coefficient of the granular ice accumulation. Eqs. (13) and (14) can be used to determine the equilibrium thickness of an ice cover formed in the wide jam mode.

During the cover progression, a simultaneous change in the flow condition takes place. A solution procedure is needed to take into consideration the interaction between the flow condition and the cover progression. Both (12) and (13) are quasi–steady-state equations that cannot be coupled with the unsteady flow equations. The interaction between the flow and the cover progression is simulated by simultaneously solving coupled quasi-steady flow and ice-thickness equations in the reach where progression takes place. This procedure is summarized in Appendix II.

Ice-Cover Stability

Cover failure can take place at any time after the formation when the internal strength is not capable of withstanding the external forces. The condition of failure of an ice cover can be formulated by considering the force balance of a section of ice cover in the longitudinal direction in a manner similar to the shoving condition. Assuming steady uniform flow and uniform cover thickness, the equilibrium condition is represented by (13). For the cover to fail, the condition to be satisfied is:

$$2(\tau_c h_0 + \mu_1 f) < (\tau_i + \tau_g + \tau_a)B \quad \text{(15)}$$

Michel (1984) pointed out that it takes only a little freezing to form a solid crust near the top surface of the ice cover to prevent the failure of the cover. Considering that the ice cover consists of a granular accumulation with a solid ice crust near the top surface and a layer of frazil deposit on its underside, the allowable longitudinal force on the ice cover, f, can be expressed in terms of strength of ice-cover layers.

$$f = f_i + f_n + f_f \quad \text{(16)}$$

in which subscripts i, n, and f = contributions from the solid crust, the granular layer, and the frazil ice layer, respectively. When a section of ice cover fails, the fragmented ice pieces may accumulate into a new cover with a larger thickness, when the flow condition permits.

Undercover Deposition and Erosion

Both surface ice particles swept under the cover at the leading edge and the suspended ice in the flow can form accumulations on the underside of the ice cover. Undercover accumulation can occur when ice particles move into a slow-moving region. Critical velocity, or critical Froude number, criterion have long been accepted as a means of determining the thickness of the undercover accumulation. Field observations suggested the critical velocity varies between 0.5 and 0.9 m/s (Ashton 1986). Sun and Shen (1988) pointed out the inadequacy of the critical velocity criteria. However, in view of the lack of a better method, the critical velocity criterion is used in the present model.

Since the thickness of frazil deposits is also limited by the amount of ice being transported along the underside of the cover, it is necessary to determine the rate of ice supply from the frazil suspension. This rate is governed by the buoyancy of frazil particles and the turbulent mixing. In one-dimensional form, assuming the exchange on the bed, the mass conservation of the frazil in suspension can be written as:

$$\frac{\partial}{\partial t}(C_v A) + \frac{\partial}{\partial x}(C_v Q) = B\left(\epsilon_y \frac{\partial c}{\partial y} - V_b c\right)_{y=d_w} \quad \text{(17)}$$

in which C_v = average ice concentration in the suspension; ϵ_y = vertical mixing coefficient; V_b = buoyant velocity; c = local ice concentration; and d_w = depth of flow underneath the cover. Approximating the right-hand-side term by $-\theta_1 V_b C_v$, (17) becomes

$$\frac{DC_v}{Dt} = -\frac{B}{A}\theta_1 V_b C_v \quad \text{(18)}$$

in which θ_1 = an empirical coefficient. Eq. (18) quantifies the rate of supply to the underside of the cover from the frazil suspension.

Thermal Growth and Decay of Ice Cover

As a result of heat exchanges at the top and bottom surfaces, an ice cover will grow or decay during the winter. A one-dimensional, quasi–steady-state finite-difference model (Shen and Lal 1986) that considers growth and decay of covers composed of white ice, black ice, and frazil ice layers is used.

When there is no water in the snow cover, in the absence of frazil layer, the rate of growth of the solid ice cover can be determined by

$$\rho_i L_i \frac{dh_i}{dt} = h_{ia}(T_s - T_a) - h_{wi}(T_w - T_m) \quad \text{(19)}$$

in which h_i = black ice thickness; h_{ia} = linearized coefficient of heat exchange between air and the top surface of the cover; T_s = temperature at the top surface of the cover; and T_m = melting temperature, 0° C. The temperature T_s can be calculated from

$$T_s = \frac{\left(T_a + \frac{1}{h_{ia}}\right)\left(\frac{h_s}{k_s} + \frac{h_w}{k_w} + \frac{h_i}{k_i}\right) + \frac{T_m}{h_{ia}}}{\frac{h_s}{k_s} + \frac{h_w}{k_w} + \frac{h_i}{k_i} + \frac{1}{h_{ia}}} \quad \text{(20)}$$

in which h = thicknesses of ice-cover layers; k = thermal conductivity; and subscripts s, w, i represent snow, white ice, and black ice. When a frazil deposit exists on the underside of the cover, (19) should be replaced by the following two equations:

$$e_f \rho_i L_i \frac{dh_i}{dt} = h_{ia}(T_s - T_a) \quad \text{(21)}$$

and

$$(1 - e_f)\frac{dh_f}{dt} = -h_{wi}(T_w - T_m) \quad \text{(22)}$$

in which e_f = porosity of the frazil layer. Eq. (21) describes the rate of growth of the solid ice into the frazil layer. Eq. (22) describes the melting of the frazil layer. Eqs. (19) and (21) are valid when $T_s < T_m$. When T_s calculated from (20) is greater than T_m, melting on the top surface of the cover takes place. The surface temperature T_s is equal to T_m. The temperature in the cover remains isothermal at 0° C and thermal growth is not possible. When a snow cover is present, the melting rate of the snow cover is given by:

$$(1 - e_s)\rho_i L_i \frac{dh_s}{dt} = h_{ia}(T_m - T_a) \quad (23)$$

in which e_s = porosity of the snow cover. In the absence of the snow cover, the melting rate on the top surface of the solid ice cover is given by

$$\rho_i L_i \frac{dh_{is}}{dt} = h_{ia}(T_m - T_a) \quad (24)$$

in which $h_{is} = h_w + h_i$ is the total thickness of the solid ice.

When the snow-cover thickness is large, the bottom surface of the snow cover may sink below the water level to form snow slush (Knight 1986). As a result of surface heat loss, white ice will grow downward from the water surface.

Model Application

A computer model RICE is developed based on the formulation presented and applied to the upper Saint Lawrence River. Detailed discussions on simulation results are presented by Lal and Shen (1990). A brief summary will be presented in this section.

The upper Saint Lawrence River flows from the outlet of Lake Ontario at Kingston, Ontario to the Moses-Saunders Power Dam at Massena, New York, with a total length of 160 km. Flow and ice conditions along the river vary considerably, as described by Yapa and Shen (1986). In general, the mean flow velocity varies from 0.1 m/s in parts of the reach upstream of Brockville, to a fast-flowing reach between Ogdensburg and Leishman Point with a mean flow velocity in the order of 1.0 m/s. Further downstream, the flow velocity reduces to about 0.5 m/s in the Lake Saint Lawrence area. The Froude number varies along the river between 0.01 to 0.14 for a typical flow condition. Formation of ice covers in the river are assisted by ice booms near Ogdensburg and Cardinal, and the Iroquois Control Dam. Due to the high flow velocity, open water areas exist immediately downstream of ice booms and the control dam. These open water areas produce the frazil ice for hanging dams.

Because of the large variations in flow and ice conditions along the upper Saint Lawrence, all of the processes formulated in the model are included in the simulation. Boom and the control dam locations are used as bridging cross sections for the initiation of ice-cover progression. In the model, the river is discretized into 32 reaches. The simulation result for the winter of 1979–80 is presented. This simulation is carried out for a period of 120 days, starting from January 1, 1980, with an overall simulation time step Δt = 1 day. Smaller time steps, δt are used for water temperature, ice transport, and cover progression simulations. Time steps δt are governed by the criteria

TABLE 1. Model Parameter Values Used in Simulation

Variable (1)	Definition (2)	Value (3)
C_p	specific heat of water	4.2 kJ kg^{-1o} C^{-1}
e_c	porosity of initial cover	0.5
e_f	porosity of frazil accumulation	0.4
F_{rc}	critical Froude number for juxtaposition	0.06
F_{rm}	maximum Froude number for ice-cover progression	0.09
$h_{i,0}$	initial thickness of skim ice	0.001 m
h_{wa}	heat exchange coefficient at water-air interface	19.7 Wm^{-2o} C^{-1}
k_i	thermal conductivity of ice	2.24 Wm^{-1o} C^{-1}
k_s	thermal conductivity of snow	0.3 Wm^{-1o} C^{-1}
L_i	later heat of fusion of water	334 J g^{-1}
t_i	thickness of ice pans in juxtaposition mode	0.1 m
$T^c_{w,s}$	critical water surface temperature for skim-ice formation	0.4° C
θV_b	modified buoyant velocity of frazil ice	0.01 m sec^{-1}
u_d	critical velocity for frazil deposition	0.6 m sec^{-1}
u_e	critical erosion velocity for frazil deposition	0.7 m sec^{-1}
α_n	decay constant for ice-cover roughness coefficients	0.1
ϕ	internal friction angle	45°
ρ	density of water	1,000 kg m^{-3}
ρ_i	density of ice	917 kg m^{-3}
τ_c	cohesive component of bank shear	0.98 kPa
μ_1	ice-to-ice friction coefficient	1.28

$(u\delta t)/(\Delta x) \leq 1$. Values of model parameters are summarized in Table 1. The ice-cover roughness coefficients can vary considerably in time as well as in space. Criteria for selecting these coefficients have been discussed by Nezhikhovskiy (1964). An empirical model for resistance coefficients of ice covers in the upper Saint Lawrence River, including the blockage effect of hanging dams, was developed by Yapa and shen (1986). In the present simulation, since the hanging-dam geometry is directly simulated, the component representing the blockage effect of hanging dams is not used. Values of bed and ice-cover resistance coefficients for the winter of the 1980 simulation are summarized in Table 2. Fig. 1 compares the observed and sim-

TABLE 2. Roughness Coefficients for Sample Simulation

Reach no. (1)	Bed roughness n_b (2)	Initial cover roughness, $n_{i,i}$ (3)	Final cover roughness, $n_{i,e}$ (4)	Decay constant α_n (5)
1–11	0.033	0.008	0.008	0.1
12–15	0.023	0.010	0.008	0.1
16–17	0.028	0.030	0.013	0.4
18–20	0.039	0.020	0.008	0.4
20–22	0.019	0.020	0.013	0.4
23–24	0.021	0.020	0.013	0.4
25	0.021	0.015	0.013	0.4
26–32	0.033	0.015	0.013	0.4

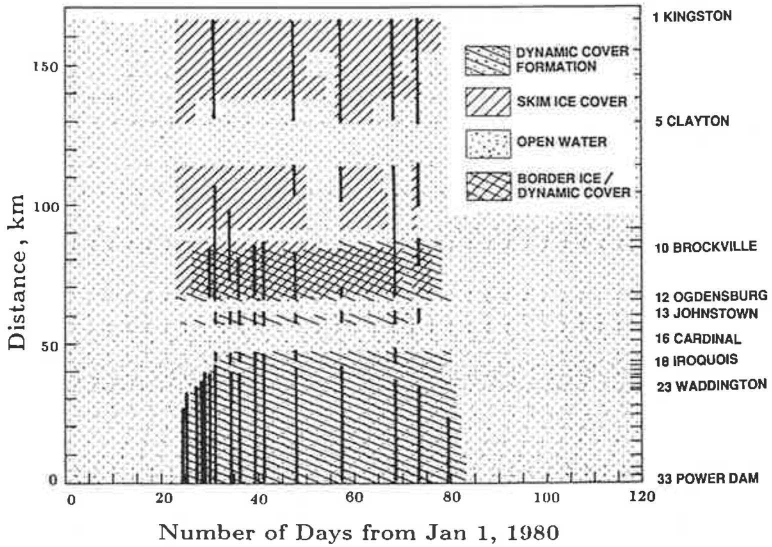

FIG. 1. Variation of Ice-Cover Distribution along River

ulated ice-cover distributions along the river. Different shades are used to represent different types of ice-cover formations. Vertical solid lines indicate observed lengths of ice covers obtained from aerial photographs. There is no aerial photograph available for reaches upstream of Iroquois before January 30 for this winter. Fig. 1 shows that the simulation agrees well with

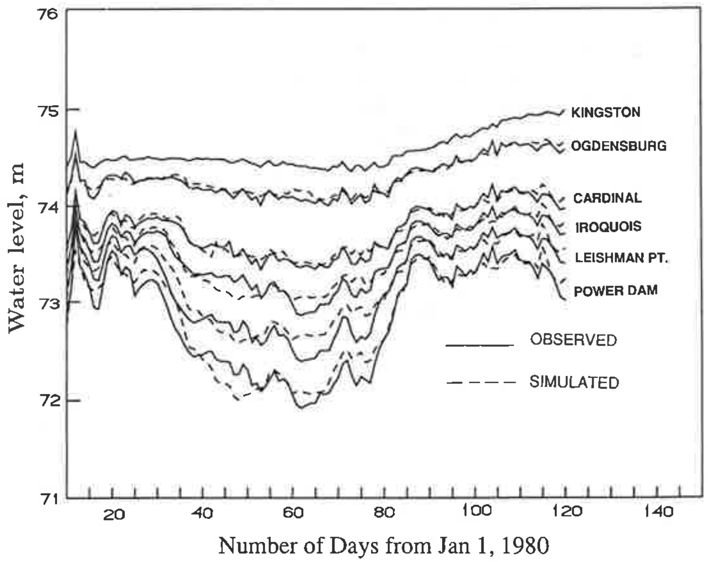

FIG. 2. Observed and Simulated Water Levels

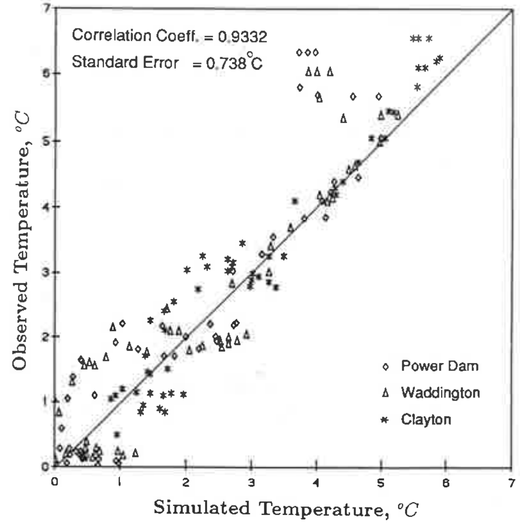

FIG. 3. Comparison of Observed and Simulated Water Temperatures, Jan. 1–Apr. 30, 1980

the observed data. In the region upstream of Brockville, the ice condition is highly nonuniform, where skim ice, juxtaposition, and jam formation often coexist in a single reach, and most of the river surface is covered by thin, unstable, static ice formation. In the Lake Saint Lawrence region, the ice cover was mainly formed in the juxtaposition mode. In the middle reach, jam formations, open waters, and hanging dams exist. Fig. 2 shows the comparison between observed and simulated water levels. This figure indicates that the model is capable of simulating water levels during both open-water and ice-covered periods. Errors in simulated water levels during the ice-covered period are larger because of the cumulative effect of errors in simulated ice-cover area, thickness, and resistance coefficients. Fig. 3 shows the comparison of observed and simulated water temperatures for stations along the river. The difference in observed and simulated water temperatures is due partially to the fact that water-temperature stations are located near the riverbank where the water temperature may not be representative of the entire cross section.

Conclusion

In this paper, a computer model is developed for simulating river ice processes in rivers with floating ice covers. The model is capable of simulating time-dependent conditions of the river hydraulics, water temperature and ice concentration, formation of snow cover, undercover accumulation and erosion, thermal growth and decay of the ice cover, and mechanical failure of the cover. A two-layer formulation is introduced to model the ice transport. In this formulation, the total ice discharge is considered to consist of the surface ice discharge and the discharge of suspended ice. The effect of surface ice on ice production as well as formations of skim ice and border ice are included. The progression and stability of the ice cover is formulated according to existing quasi-static equilibrium ice-jam theories with consideration to the interaction between the ice cover and the flow. The undercover ice accumulation is formulated according to the critical velocity criterion. The growth and decay of the ice cover is simulated using a finite-difference formulation applicable to composite ice covers consisting of snow, ice, and frazil layers. The model is applied to the upper Saint Lawrence River with good results. With the generic nature of the model structure, the model can be applied to other rivers (e.g., Shen et al. 1989). In view of the limited current understanding of river ice processes, further improvements of the model should be made when improved formulations become available. Particular attention should be given to undercover accumulation, mechanical breakup, and ice-cover roughness. Improvements on modeling techniques are also possible by including some important two-dimensional aspects of ice processes.

ACKNOWLEDGMENT

This study was supported by the River Ice Management (RIM) program of the U.S. Army Cold Regions Research and Engineering Laboratory, Hanover, New Hampshire, through Contract No. DACA 89-84-K-0008, under the Clarkson–CRREL Joint Graduate Research Program in Ice Engineering.

APPENDIX I. TWO-LAYER ICE TRANSPORT

The ice discharge in the river is considered to consist of a surface layer and a suspended layer. The surface layer is assumed to have a thickness equal to the thickness of surface ice elements, and is negligible compared to the flow depth. The suspended layer is assumed to extend approximately over the entire depth. Volumetric rates of ice transport in these two layers are given by the following expressions:

$$Q_s^i = [h_i + (1 - e_f)h_f]C_a B_0 U \quad (25)$$

$$Q_d^i = C_v AU \quad (26)$$

in which Q_s^i, Q_d^i = volumetric rate of ice discharges in surface and suspended layers, respectively; h_i = solid ice thickness in floating surface ice elements; h_f = thickness of frazil ice layer on the underside of surface ice elements; e_f = porosity of the frazil ice layer; C_a = area concentration or the fraction of water surface area covered by surface ice elements; C_v = average volumetric concentration of frazil ice in the suspended layer. The velocity of surface ice is assumed to be the same as the mean flow velocity U.

For the surface layer, the equation of mass conservation can be written as follows:

$$\frac{\partial}{\partial t}\{[h_i + (1 - e_f)h_f]C_a B_0\} + \frac{\partial}{\partial x}\{[h_i + (1 - e_f)h_f]C_a B_0 U\} = \frac{B_0 C_a \phi_{si}}{\rho_i L} + E \quad (27)$$

Similarly, for the suspended layer, the equation of mass conservation is:

$$\frac{\partial}{\partial t}(C_v A) + \frac{\partial}{\partial x}(C_v AU) = \frac{B_0(1 - C_a)\phi_{sw}}{\rho_i L} - D - E \quad (28)$$

in which ϕ_{si} = net rate of heat loss per unit area over the surface of floating ice elements; ϕ_{sw} = net rate of heat loss per unit area over the open-water portion of the water surface; and D, E = net exchange of ice flux at the bed and the interface between the surface and the suspended layers, respectively. Longitudinal dispersion of both volumetric and surface concentrations are neglected by assuming that concentration gradients are small.

Assuming that the rate of the exchange between the surface and the suspended layers, E/B, can be represented by $\theta V_b C_v$. The value of θ should decrease with the increase in the intensity of vertical mixing at the water surface. When this vertical mixing is negligible, the value of θ approaches 1.0. Neglecting the exchange at the bed, D, (27) and (28) become:

$$A\frac{DC_v}{Dt} = \frac{B_0\phi_{sw}(1 - C_a)}{\rho_i L} - \theta V_b C_v B_0 \quad (29)$$

$$C_a B_0 \frac{D}{Dt}[h_i + (1 - e_f)h_f] + [h_i + (1 - e_f)h_f]\frac{D}{Dt}(C_a B_0) = \frac{B_0 C_a \phi_{si}}{\rho_i L} + \theta V_b C_v B_0 - hC_a B_0 \frac{\partial u}{\partial x} \quad (30)$$

in which V_b = buoyant velocity of frazil ice; and θ = an exchange coefficient at the interface between the suspended and surface layers. The value of V_b varies with the size of the frazil. For a frazil diameter of 1 mm, the buoyant velocity is about 0.01 m/s.

By assuming that the heat loss over surface ice elements is responsible for the growth of the solid ice thickness, the rate of change of solid ice thickness can be obtained:

$$\frac{Dh_i}{Dt} = \frac{\phi_{si}}{e_f \rho_i L} \quad (31)$$

The rate of change of frazil ice thickness depends on the rate of frazil ice deposition on the underside of ice pans, and the rate of downward growth of solid ice into the frazil ice deposit.

$$\frac{Dh_f}{Dt} = \frac{\theta V_b C_v}{(1 - e_f)} - \frac{Dh_i}{Dt} \quad (32)$$

Using (31) and (32) or their equivalent, (30) can be further reduced to:

$$[h_i + (1 - e_f)h_f]\frac{D}{Dt}(C_0 B_0) = (1 - C_a)\theta V_b C_v B_0 - [h_i + (1 - e_f)h_f]C_a B_0 \frac{\partial u}{\partial x} \quad (33)$$

Solution of variables h_i, h_f, C_v and C_a can be obtained from (29), (31), (32), and (33). Since V_b always appears with θ, and there is no analytical means to determine their values accurately, the product θV_b can be considered a single parameter. Both ice pieces in the surface layer and frazil ice in the suspended layer are mixtures of particles of different sizes. These size distributions are not considered. Values of h_f, h_i and θV_b can be considered as weighted average values for these mixtures.

Appendix II. Calculation of Initial Cover Thickness

For progression in the juxtaposition mode, the initial cover thickness equals the thickness of surface ice elements, t_i. It is necessary, however, to calculate F_r at the front of progressing cover to compare with F_{rc}. Assuming the progression takes place in a reach Δx_i, the total head at the upstream end of this reach can be written as:

$$\left(H + \frac{Q^2}{2gA^2}\right) = H_0 + \frac{Q^2}{2gA_0^2} + \bar{S}_f \Delta x_i \quad (34)$$

in which H = water level; $\bar{S}_f$ = average energy slope; and the subscript 0 = the downstream end of the reach, where the flow condition is known. Eq. (34) can be used to solve for A and H, and hence F_r.

In the hydraulic thickening mode, the initial cover thickness can be calculated from (12), which can be written as:

$$Q^2 - 2gA^2\left(1 - \frac{\rho_i}{\rho}\right)h_0 = 0 \quad (35)$$

Using the Newton-Raphson algorithm, (34) and (35) can be solved simultaneously for A and h_0.

In the mechanical thickening mode, (13) can be written as:

$$\mu \frac{\rho_i}{\rho}\left(1 - \frac{\rho_i}{\rho}\right)h_0^2 + \frac{2\tau_c h_0}{\rho g} - 2^{1/3}\frac{Q^2 n_c^2 B_0^{4/3}}{A^{7/3}}$$
$$\left[\left(\frac{n_i}{n_c}\right)^{3/2} + 2\frac{\rho_i}{\rho}\frac{h_0 B_0}{A}\right] - \frac{B_0 \tau_a}{\rho g} = 0 \quad (36)$$

in which $\mu = \mu_1 K_2$; n_c = composite Manning's coefficient, $[(n_i^{3/2} + n_b^{3/2})/2]^{2/3}$. The simultaneous solution of (34) and (36) gives A and h_0.

Appendix III. References

Ashton, G. D., ed. (1986). *River and lake ice engineering*. Water Resources Publications, Littleton, Colo.

Calkins, D. J. (1984). "Numerical simulation of freeze-up on the Ottaquechee River." *Proc. of the 3rd Workshop on the Hydraulics of River Ice*, Univ. of New Brunswick, Fredericton, New Brunswick, Canada, 247–277.

Kivisild, H. R. (1959). "Hydrodynamical analysis of ice floods." *Proc., IAHR 8th Congress*, Vol. III, International Association for Hydraulic Research.

Knight, C. A. (1986). "Slush on lakes." *Structure and dynamics of partially solidified systems*, Martinus Nijhoff Publishers, Brussels, Belgium, 455–465.

Lal, A. M. W. (1989). "A mathematical model for river ice processes," thesis presented to Clarkson University, at Potsdam, N.Y., in partial fulfillment of the requirements for the degree of doctor of philosophy.

Lal, A. M. W., and Shen, H. T. (1990). "A mathematical model for river ice processes (RICE)." *CRREL Report 465*, U.S. Army Cold Regions Res. and Engrg. Lab., Hanover, N.H.

Matousek, V. (1984). "Types of ice run and conditions for their formation." *Proc., IAHR Symposium on Ice*, Vol. 1, International Association for Hydraulic Research, 316–327.

Matousek, V. (1988). "Hypothesis of dynamic ice bridge formation." *Proc. IAHR Ice Symposium*, International Association for Hydraulic Research, 249–260.

Michel, B. (1984). "Comparison of field data with theories on ice progression in large rivers." *Can. J. Civ. Engrg.*, Vol. 11(5), 789–814.

Michel, B., Marcotte, N. Fonseca, F., and Rivard, G. (1982). "Formation of border ice in the Ste. Anne River." *Proc. of the Workshop on Hydraulics of Ice-Covered Rivers*, Univ. of Alberta, Edmonton, Alberta, Canada, 38–61.

Nezhikhovskiy, R. A. (1964). "Coefficient of roughness of bottom surfaces of slush ice cover." *Soviet hydrology, Selected papers*, 2, 127–150.

Petryk, S., Panu, U., Kartha, V. C., and Clement, F. (1981). "Numerical modelling and predictability of ice regime in rivers." *Proc., IAHR International Symposium on Ice*, Vol. 1, 426–436.

Pariset, E., and Hausser, R. (1961). "Formation and evolution of the ice covers on rivers." *Engrg. Inst. of Canada, Trans.*, 5(1), 41–49.

Shen, H. T., and Chaing, L. A. (1984). "Simulation of growth and decay of river ice cover." *J. Hydr. Div.*, ASCE, 110(7), 958–971.

Shen, H. T., and Lal, A. M. W. (1986). "Growth and decay of river ice covers." *Proc., Cold Regions Hydro. Symp.*, American Water Resources Association, 583–591.

Shen, H. T., and Yapa, P. D. (1984). "Computer simulation of the ice cover formation in the upper St. Lawrence River." *Proc. of the 3rd Workshop on the Hydraulics of River Ice*, Univ. of New Brunswick, Fredericton, New Brunswick, Canada, 227–246.

Shen, H. T., Ruggles, R. W., and Batson, G. B. (1984). "Field investigation of St. Lawrence River hanging ice dams, winter of 1983–1984." *Report No. DTSL55-84-C0085A*, U.S. Dept. of Transp., Washington, D.C.

Shen, H. T., Shen, H. H., and Tsai, S. M. (1990). "Dynamic transport of river ice." *J. Hydr. Res.*, 28(6), 659–671.

Shen, H. T., Bjedov, G., Daly, S. F., and Lal, A. M. W. (1989). "A numerical model for Ohio River ice conditions." *Report 88-4*, Dept. of Civ. and Envir. Engrg., Clarkson Univ., Potsdam, N.Y.

Sun, Z. C., and Shen, H. T. (1988). "A field investigation of frazil ice jam in Yellow River." *Proc. of the 5th Workshop on Hydraulics of River Ice/Ice Jams*, NRC of Canada, Winnipeg, Canada, 157–175.

Svensson, U., Billfalk, L., and Hammar, L. (1989). "A mathematical model of border-ice formation in rivers." *Cold Reg. Sci. Tech.*, 16(2), 179–189.

Yapa, P. D., and Shen, H. T. (1986). "Unsteady flow simulation for an ice-covered river." *J. Hydr. Div.*, ASCE, 112(11), 1036–1049.